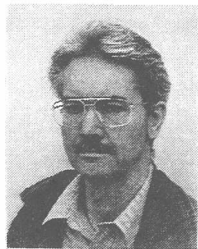


DIFFRACTIVE PRODUCTION OF $\rho^0(770)$ IN
MUON-PROTON SCATTERING AT 470 GEV

Wolfgang Wittek (representing the E665 Collaboration)
Max-Planck-Institut für Physik (Werner-Heisenberg-Institut)
Föhringer Ring 6, D-80805 Munich, Germany
e-mail: wittek@mppmu.mpg.de



Abstract

The diffractive production of $\rho^0(770)$ mesons in the reaction $\mu^+p \rightarrow \mu^+\rho^0p$ is studied using data of the E665 experiment. The experiment covers the kinematic region $0.15 \text{ GeV}^2 < Q^2 < 10 \text{ GeV}^2$, $8 \text{ GeV} < W < 25 \text{ GeV}$. Results are presented on the $\pi^+\pi^-$ mass spectrum, on the Q^2 and W dependence of the cross section for ρ^0 production by virtual photons, and on the Q^2 dependence of the production and decay angular distributions of the ρ^0 . The data show typical features of a soft diffractive process.

In this analysis the diffractive production of $\rho^0(770)$ mesons in the reaction



is studied. The data were taken in a fixed target run of the E665 experiment at the Tevatron at Fermilab. Candidates of reaction (1) are selected by requiring the presence in the final state of two and only two observed hadrons of opposite charge (the decay pions of the ρ^0), which carry at least 90% of ν , the energy of the virtual photon (γ^*) in the laboratory frame. In addition, $t' = t - t_{\min}$, where t is the negative four-momentum transfer squared from the virtual photon to the target proton, has to be less than 1 GeV^2 . Corrections are computed using a Monte Carlo program in which both non-diffractive and diffractive events are simulated. The corrections allow for trigger and reconstruction inefficiencies, measurement errors, misidentifications and radiative effects, for the background from non-diffractive events, and for the background from diffractive events in which the target proton dissociates (double-difraction dissociation). Absolute cross sections are determined by normalizing to the reaction



where H denotes any hadronic system. The cross section for reaction (2) was measured in the same experiment [1].

Further details about the detector, the triggers, the data taking, the event processing, reconstruction and selection, the Monte Carlo simulation of the experiment, the method of correcting the data and the procedure of determining absolute cross sections can be found in [2, 1, 3]. In the following only fully corrected results will be presented.

Fig. 1 shows for different regions of $\log_{10}(Q^2/\text{GeV}^2)$ the distribution of the effective mass M_X of the two charged hadrons. Besides the ρ^0 bump there is a clear signal of $\phi(1020)$ production. Fits of a relativistic P-wave Breit-Wigner function for the ρ^0 , which contained a mass skewing factor of the form $(M_\rho/M_X)^n$, to the mass distributions in Fig. 1 indicate a decrease of n and thus a diminution of the asymmetry of the ρ^0 mass distribution as Q^2 increases. The asymmetry can be related to a corresponding behavior of the $\pi^+\pi^-$ mass spectrum in e^+e^- annihilation [4, 3]. A Q^2 dependence of the asymmetry is predicted by the vector meson dominance model [5, 4]. The mass skewing parameter n , averaged over the whole Q^2 range, is $n = 3.73 \pm 0.27$.

As expected for a diffractive process, the distribution of t' for the $\pi^+\pi^-$ mass region 0.57 to 0.97 GeV exhibits an exponential decrease. Fits of the expression $a \cdot e^{-bt'}$ to the t' distributions in different regions of $\log_{10}(Q^2/\text{GeV}^2)$ (Fig. 2) yield slope values b which decrease as Q^2 increases. This implies a shrinkage of the effective γ^*p interaction radius with increasing Q^2 . The slope value b , as determined in the region $0 < t' < 0.5 \text{ GeV}^2$ and averaged over the whole Q^2 range, is $b = (7.0 \pm 0.2 \text{ (stat.)} \pm 0.2 \text{ (syst.)}) \text{ GeV}^{-2}$.

Within the ν range covered by this analysis, no dependence of b on ν (or W , the effective mass of the system formed by the virtual photon and the target proton) is observed. However, a W dependence is suggested by comparing the E665 measurement $b = (7.7 \pm 0.4 \text{ (stat.)} \pm 0.3 \text{ (syst.)}) \text{ GeV}^{-2}$ for $t' < 0.5 \text{ GeV}^2$, $0.32 \text{ GeV}^2 < Q^2 < 0.56 \text{ GeV}^2$ and $8 \text{ GeV} < W < 25 \text{ GeV}$

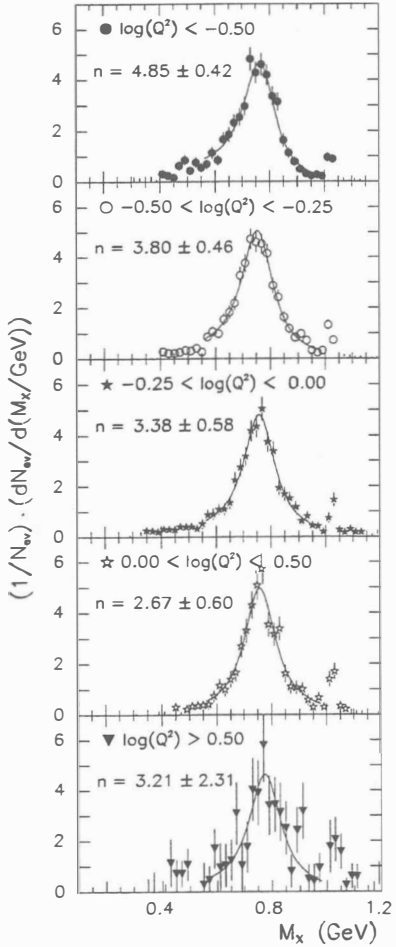


Figure 1: Distributions of the h^+h^- effective mass M_X in different regions of $\log_{10}(Q^2/\text{GeV}^2)$. The curves represent the results of the fits of a relativistic P-wave Breit-Wigner function, which includes a mass skewing factor, to the mass distributions in the mass range $0.56 \text{ GeV} < M_X < 0.98 \text{ GeV}$. The fitted value of the exponent n in the mass skewing factor is given for each Q^2 bin. The errors shown are statistical.

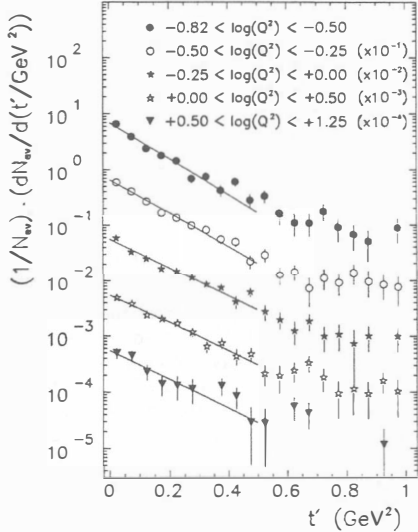


Figure 2: t' distributions in different regions of $\log_{10}(Q^2/\text{GeV}^2)$, corrected to exclude the full double-diffraction contribution. The solid lines represent the results of fits of the expression $a \cdot e^{-bt'}$ to the experimental distributions. The errors shown are statistical.

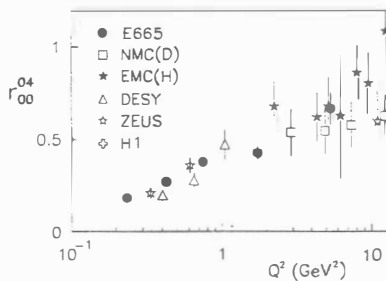


Figure 3: The spin density matrix element r_{00}^{04} as a function of Q^2 . Previous measurements from DESY [8], EMC [9], NMC [10], ZEUS [11, 6] and H1 [12] are shown for comparison. The errors on the E665 data points are statistical.

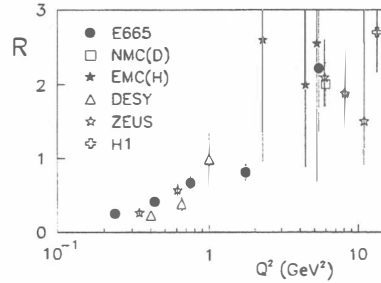


Figure 4: $R = \sigma_L/\sigma_T$ as determined from the measured values of r_{00}^{04} , plotted as a function of Q^2 . Previous measurements from DESY [8], EMC [9], NMC [10], ZEUS [11, 6, 13] and H1 [12] are shown for comparison. The errors on the E665 data points are statistical.

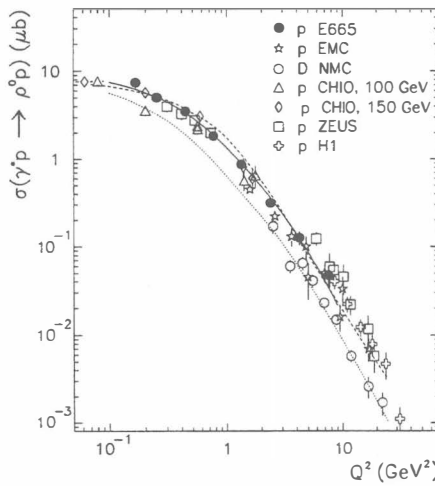


Figure 5: $\sigma(\gamma^* p \rightarrow \rho^0 p)$ as a function of Q^2 : E665 data (full circles) and the results from the CHIO [19], EMC [20], NMC [10], H1 [12] and ZEUS [11, 6, 13] experiments. The solid line represents the result of fitting expression (4) to the E665 data points. The dashed line is a prediction by Pichowsky et al. [18] for $W = 15$ GeV and $\epsilon = 1$. The dotted line is the prediction by J. Nemchik et al. [17] for $W = 15$ GeV and $\epsilon = 1$. The errors on the E665 data points are statistical. The systematic error of the E665 cross sections is in the order 20% [3].

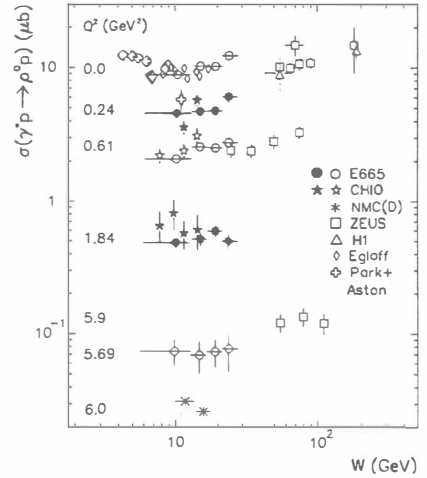


Figure 6: $\sigma(\gamma^* p \rightarrow \rho^0 p)$ as a function of W in different ranges of Q^2 . The numbers in the plot denote the approximate values of Q^2 . The data in the various Q^2 ranges are alternately represented by open and full symbols. The data for $Q^2 > 0$ are from this experiment (E665, circles), from the CHIO [19], the NMC [10, 23] and the ZEUS [11, 6, 13] experiments. The photoproduction data ($Q^2 = 0$) are from [24, 21, 22] and from the ZEUS [25, 26, 27] and H1 [28] experiments. The E665 data points at $Q^2 = 0$ represent the extrapolated cross sections σ_0 . The errors on the E665 data points are statistical. The systematic error of the E665 cross sections is in the order 20% [3].

with the preliminary result $b = (9.3 \pm 0.7 \text{ (stat.)} \pm 0.8 \text{ (syst.)}) \text{ GeV}^{-2}$ for $t < 0.4 \text{ GeV}^2$, $0.25 \text{ GeV}^2 < Q^2 < 0.85 \text{ GeV}^2$ and $50 \text{ GeV} < W < 90 \text{ GeV}$ from the ZEUS experiment [6]. In the framework of the Regge theory with pure Pomeron exchange the observed increase of b with W is consistent with a slope α' of the Pomeron trajectory of $\alpha' = \Delta b/(4\Delta \ln W) \approx 0.25 \text{ GeV}^{-2}$, which is typical for a soft Pomeron [7].

The production and decay angular distributions of the ρ^0 were used to determine some elements of the spin density matrix, which describes the spin state of the ρ^0 . It is found that the fraction of longitudinally polarized ρ^0 , given by the matrix element r_{00}^{04} , increases from 0.182 ± 0.027 at low Q^2 to 0.672 ± 0.086 at high Q^2 (Fig. 3).

The hypothesis of s-channel helicity conservation (SCHC) and natural-parity exchange in the t-channel implies vanishing spin-density matrix elements r_{1-1}^{04} and r_{1-1}^3 and a relation between r_{00}^{04} and r_{1-1}^1 . In all cases the data were consistent with these predictions.

Assuming SCHC, the ratio $R = \sigma_L/\sigma_T$ of cross sections for ρ^0 production by longitudinally or transversely polarized virtual photons follows from r_{00}^{04} by $R = r_{00}^{04}/(\epsilon \cdot (1 - r_{00}^{04}))$, where ϵ is the ratio of fluxes of longitudinally and transversely polarized virtual photons. R is displayed in Fig. 4 as a function of Q^2 . R rises with Q^2 , which is qualitatively predicted by most of the models on diffractive leptoproduction of ρ^0 [14, 15, 16, 17, 18].

The cross section $\sigma(\gamma^* p \rightarrow \rho^0 p) = \sigma_T + \epsilon \sigma_L$ was determined via the relation

$$\sigma(\gamma^* p \rightarrow \rho^0 p) = \frac{1}{\Gamma_T} \cdot \frac{d\sigma(\mu p \rightarrow \mu \rho^0 p)}{d\nu dQ^2}, \quad (3)$$

where Γ_T is the flux of transverse photons. It is plotted in Fig. 5 as a function of Q^2 . The solid curve represents the result of a fit of the expression

$$\sigma = \sigma_0 \left(\frac{M_\rho^2}{Q^2 + M_\rho^2} \right)^m \cdot [1 + \epsilon \cdot R(Q^2)] \quad (4)$$

to the E665 data points (full circles), where σ_0 and m were treated as free parameters and $R(Q^2)$ was taken from an interpolation of the E665 data points in Fig. 4. The result for the exponent m is $m = 2.51 \pm 0.07$, which is larger than the prediction ($m = 2$) from the vector dominance model. σ_0 , which can be regarded as an estimate of the photoproduction cross section, is determined as $\sigma_0 = (10.23 \pm 0.56) \mu\text{b}$, which is in good agreement with direct measurements in photoproduction experiments [21, 22]. The dotted and dashed curves are predictions of the models from [17] and [18] respectively, for $W = 15 \text{ GeV}$ and $\epsilon = 1$.

The W dependence of $\sigma(\gamma^* p \rightarrow \rho^0 p)$ at fixed Q^2 is investigated in Fig. 6. In the E665 kinematic range $8 \text{ GeV} < W < 25 \text{ GeV}$ the cross section $\sigma(\gamma^* p \rightarrow \rho^0 p)$ is nearly constant. A comparison with the results from the ZEUS experiment [11, 6, 13] at higher W suggests a weak increase with W , which appears to be stronger at higher Q^2 .

In summary, the reaction $\gamma^* p \rightarrow \rho^0 p$ in the kinematic region $0.15 \text{ GeV}^2 < Q^2 < 10 \text{ GeV}^2$, $8 \text{ GeV} < W < 25 \text{ GeV}$ exhibits typical features of a soft diffractive process: an exponential decrease of the cross section in t' , approximate s-channel helicity conservation, and a rise of R

with Q^2 . The softness of the reaction is reflected in the weak shrinkage of the t' distribution as W increases and in the weak W dependence of the cross section at fixed Q^2 .

References

1. M.R. Adams et al., Phys. Rev. D54 (1996) 3006
2. M.R. Adams et al., Nucl. Inst. and Meth. A291 (1990) 533
3. M.R. Adams et al., Diffractive production of $\rho^0(770)$ mesons in muon-proton interactions at 470 GeV, MPI-PhE/97-03, paper submitted to Z. Phys. C (1997)
4. G. Niesler et al., Phys. Lett. B389 (1996) 157
5. R. Ross and L. Stodolsky, Phys. Rev. 149 (1966) 1172
6. O. Lukina (ZEUS), Ref. pa 02-053, Contribution to the XXVIII Conference on High Energy Physics, Warsaw, 1996
7. A. Donnachie and P.V. Landshoff, Phys. Lett. B348 (1995) 213
8. P. Joos et al., Nucl. Phys. B113 (1976) 53
9. J.J. Aubert et al. (EMC), Phys. Lett. 161B (1985) 203
10. M. Arneodo et al. (NMC), Nucl. Phys. B429 (1994) 503
11. M. Derrick et al. (ZEUS), Phys. Lett. B356 (1995) 601
12. S. Aïd et al. (H1), Nucl. Phys. B468 (1996) 3
13. J. Bulmahn (ZEUS), Ref. pa 02-028, Contribution to the XXVIII Conference on High Energy Physics, Warsaw, 1996
14. T.H. Bauer et al., Rev. Mod. Phys. 50 (1978) 261
15. A. Donnachie and P.V. Landshoff, Phys. Lett. B185 (1987) 403
16. S.J. Brodsky et al., Phys. Rev. D50 (1994) 3134
17. J. Nemchik et al., DFTT71/95, KFA-IPK (TH)-24-95, hep-ph/9605231
18. M.A. Pichowsky and T.-S.H. Lee, ANL-PHY-8529-TH-96, nucl-th/9612049
19. W.D. Shambroom et al. (CHIO), Phys. Rev. D26 (1982) 1
20. J. Ashman et al. (EMC), Z. Phys. C39 (1988) 169
21. R.M. Egloff et al., Phys. Rev. Lett. 43 (1979) 657
22. D. Aston et al., Nucl. Phys. B209 (1982) 56
23. M. Arneodo et al. (NMC), Il Nuovo Cim. 108A (1995) 1247
24. J. Park et al., Nucl. Phys. B36 (1972) 404
25. M. Derrick et al. (ZEUS), Z. Phys. C63 (1994) 391
26. M. Derrick et al. (ZEUS), Z. Phys. C69 (1995) 39
27. ZEUS Collaboration, Ref. pa 02-050, Contribution to the XXVIII Conference on High Energy Physics, Warsaw, 1996
28. S. Aïd et al. (H1), Nucl. Phys. B463 (1996) 3

HEAVY IONS

